

We investigated the kinetic properties of the hyperpolarization-activated inward current ( $I_h$ ) of thalamocortical (TC) neurons. Recently, it was shown that this current is characterized by different time constants of activation and inactivation, which was in apparent conflict with the single-exponential time course of the current. We introduce here a model of  $I_h$  based on the cooperation of a slow and a fast activation variable and show that this kinetic scheme accounts for these apparently conflicting experimental data. We also report that following the combination of such a current with other currents seen in TC cells, one observes several types of oscillating behavior, similar to the slow oscillations and the spindle-like oscillations seen *in vitro*.

**Key words:** Thalamus; Sleep; Lateral geniculate nucleus; Biophysical model; Hodgkin-Huxley formalism; Slow oscillations; Spindle-like oscillations; Low-threshold calcium current; Inward rectifier; Potassium currents

## A model of the inward current $I_h$ and its possible role in thalamocortical oscillations

A. Destexhe<sup>CA</sup> and A. Babloyantz

Université Libre de Bruxelles, CP 231–Campus Plaine, Boulevard du Triomphe, B-1050 Bruxelles, Belgium; <sup>1</sup> The Salk Institute, Computational Neurobiology Laboratory, 10010 North Torrey Pines Road, La Jolla, CA-92037, USA

<sup>CA</sup> Corresponding Author

### Introduction

During wakefulness, the essential role of thalamocortical (TC) neurons is to provide an efficient relay of incoming sensory information towards the cortex. During synchronized sleep, the same neurons are characterized by several types of membrane potential oscillations which render thalamic neurons considerably less receptive to other stimuli. It is believed that the onset of this oscillatory mode depends both on network properties and the modulation of intrinsic currents in these neurons.<sup>1</sup>

The study of electrophysiological properties of single TC neurons *in vitro* reveals several types of spontaneous oscillations. Slow oscillations (0.5–2.9 Hz) are commonly seen in cat and rat TC neurons<sup>2,3</sup> and constitute the spontaneous activity of some of these neurons *in vitro*. Similar slow oscillations have been observed *in vivo* in TC neurons during slow wave sleep.<sup>4</sup> Another type of oscillating behavior, termed spindle-like oscillations, has also been observed in cat TC cells *in vitro*.<sup>3</sup> These oscillations are characterized by bursts of slow oscillations (0.5–3.2 Hz), separated by relatively long periods (5–25 s) during which the membrane is silent and hyperpolarizes slowly. However, these oscillations differ significantly from the oscillations recorded *in vivo* during sleep spindles, which originate probably in the reticular nucleus.<sup>5</sup>

Voltage-clamp studies of TC neurons revealed the presence of several currents which are thought to be responsible for these oscillations. First, the low-threshold calcium current  $I_T$ , initially described by Jahnsen and Llinas,<sup>6</sup> recently was fully characterized.<sup>7</sup> Another current which was shown to be of central importance for oscillating behavior is the hyperpolarization-activated inward current  $I_h$ , characterized by McCormick and Pape.<sup>2</sup> Several potassium currents

have also been described<sup>8–11</sup> and might have an important role in oscillatory behaviour.

In this paper, we focus on the kinetic description of the inward current  $I_h$ , as described by voltage clamp experiments by McCormick and Pape.<sup>2</sup> The essential features of this current are that it is noninactivating and it is activated by hyperpolarization below threshold. It also has unusual kinetic properties. At a given membrane potential, the time constant of activation may be different from the time constant of deactivation, which suggests complex kinetics. This observation is not consistent with the single exponential time course of  $I_h$ , which suggests a simple kinetic scheme. We introduce here a kinetic scheme that accounts for voltage-clamp data and explains this apparent contradiction. We also investigate the oscillatory behavior seen in a single compartment model of the TC cell, including this model of  $I_h$  as well as other currents.

### Materials and Methods

In all simulations presented here, the cell is considered as a single compartment, and the variations of the membrane potential are obtained through the numerical resolution of kinetic equations following the standard Hodgkin-Huxley scheme.<sup>12</sup>

For simulating voltage-clamp experiment on  $I_h$ , the equation used is:

$$I_h = \bar{g}_h F S (V - V_h) \quad [1]$$

where  $V$  is the membrane potential at which the cell is clamped (in mV),  $\bar{g}_h$  is the maximal conductance of  $I_h$  (in mS/cm<sup>2</sup>),  $V_h = -43$  mV is the reversal potential of  $I_h$ ,<sup>2</sup>  $S$  and  $F$  are the activation variables associated to this current. These variables are described by the following first-order equations:

$$\frac{dF}{dt} = (H_x(V) - F) / \tau_F(V) \quad [2]$$

$$\frac{dS}{dt} = (H_x(V) - S) / \tau_S(V) \quad [3]$$

where the activation function  $H_x(V)$  is estimated such as  $H^{\infty}$  fits the data points obtained in reference 2 (see Table 1). The time constants  $\tau_F(V)$  and  $\tau_S(V)$  are estimated from numerical simulation of voltage clamp protocols (cf Results section and Table 1).

For simulating membrane potential oscillations, the following equation is used:

$$C_m \frac{dV}{dt} = -g_L(V - V_L) - I_T - I_b - I_{K2} \quad [4]$$

where  $C_m = 1 \mu\text{F}/\text{cm}^2$  is the specific capacity of the membrane,  $g_L = 0.05 \text{ mS}/\text{cm}^2$  and  $V_L = -85 \text{ mV}$  are respectively the leakage conductance and the leakage potential.  $g_L$  is estimated such as to get a time constant of 20 ms, and  $V_L$  is adjusted such as to obtain a reasonable value of the membrane potential, in the range of  $-70$  to  $-60 \text{ mV}$ .<sup>13</sup>  $I_T$  represents the low-threshold calcium current, characterized by Coulter *et al.*,<sup>7</sup> and  $I_{K2}$  represents the slow potassium current, characterized by Huguenard and Prince.<sup>9</sup> For these two currents, models have been developed and the same models will be used here (cf. reference 14 for  $I_T$ , and reference 15 for  $I_{K2}$ ). As in the experiments of McCormick and Pape,<sup>2</sup> the temperature is set to  $36^\circ\text{C}$  by assuming  $Q_{10}$  values of 5 and 3 for  $I_T$ ,<sup>7</sup> and of 2.6 for  $I_{K2}$ .<sup>9</sup> The screening charge effect is calculated assuming an extracellular calcium concentration of 2 mM (cf reference 14).

Conductance values and reversal potentials are estimated from the literature. However, it must be pointed out that, for each one of the three currents considered here, the value of the maximal conductance and the reversal potential are interrelated. For example, if  $V_b$  is increased,  $\bar{g}_b$  must be decreased to recover similar type of behavior. Therefore, as these parameters are not known with high accuracy, a broad range of these values must be tested. The values of maximal conductances given in the following must be considered as representative of the system, and we verified that similar type of behavior is obtained for a wide range of these parameters.

The differential equations were integrated numerically, using a fifth order, variable-step integration subroutine, provided by the CERN library (MERSON D208) with a fixed accuracy of 0.00001%. The minimal integration step was of the order of  $10^{-2}$  to  $10^{-3}$  ms.

Comparison between single and double precision results showed that single precision is sufficient for integration of equations 1–4.

All numerical integrations were performed using Fortran 77 and C programming languages. Sony NWS 3410, Apollo 400 or MIPS 3000 workstations were used. The typical time taken by a simulation of 10 s was of the order of 8–12 s CPU time.

## Results

Voltage-clamp experiments<sup>2</sup> show that time constants of  $I_b$  obtained during activation may be considerably different from that measured from deactivation at the same membrane potential. On activation, rather slow time constants were seen whereas deactivation appeared to proceed much faster. Only complex kinetic schemes may account for such data. On the other hand, the time course of  $I_b$  follows a single exponential and suggests a simple kinetic description involving one activation variable. In this latter case, however, time constants of activation must be rigorously identical to those of inactivation.

One possible way of solving this conflict is by considering double activation kinetics for  $I_b$ . Let us assume that two distinct activation variables characterize the kinetics of  $I_b$ , namely  $F$  (fast activation) and  $S$  (slow activation), such that the current is proportional to the product  $SF$ . These activation variables are characterized by the same activation function, and by time constants of different magnitudes.

During activation, the two variables  $S$  and  $F$  are initially close to zero. As the voltage is clamped to a value where  $S$  and  $F$  activate, the fast variable  $F$  rapidly increases to its stationary value whereas  $S$  reaches the same value much more slowly. As  $I_b$  is proportional to the product  $SF$ , the time course of the measured current will essentially follow the activation kinetics of the variable  $S$  (Fig. 1a). On the other hand, in a deactivation experiment, the two variables are initially close to 1. When the voltage is clamped to a value where  $S$  and  $F$  deactivate, the same scenario as above is seen:  $F$  rapidly reaches its stationary value whereas  $S$  decreases more slowly. In this case, however, the initial decrease of  $F$  will also lead to an immediate decrease of  $I_b$ . Therefore, on deactivation, the time course of the measured current will essentially follow the kinetics of the fast variable (Fig. 1b).

A simulation of voltage-clamp experiments on  $I_b$  (Fig. 1a–b) shows that the time course of current corresponds to a sum of two exponentials. However, usually only one component is prominent in this sum, so the current can be fitted with a single exponential. This could explain the apparent single exponential curves observed experimentally. Figure 1c shows that such a two variable activation kinetic scheme may account for the difference between activation and deactivation kinetics. Although it does not account rigorously for all ex-

**Table 1.** Activation function and time constants of  $I_b$

Function name	Function value
Activation function	$H_x(V) = 1/(1 + \exp[(V + 68.9)/6.5])$
Slow time constant	$\tau_S(V) = \exp[(V + 183.6)/15.24]$
Fast time constant	$\tau_F(V) = \exp[(V + 158.6)/11.2]/(1 + \exp[(V + 75)/5.5])$

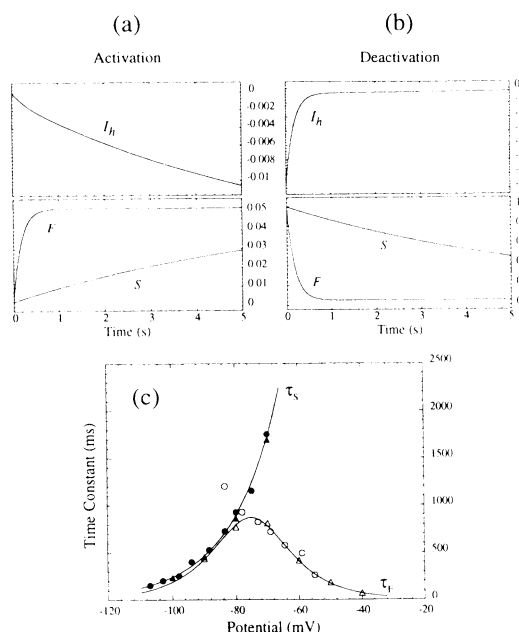


FIG. 1. Simulation of voltage clamp protocols on the double activation model of  $I_h$ . (a) activation of  $I_h$ . The voltage is initially of  $-30$  mV and the current is recorded after the voltage is clamped to  $-50$  mV. Time courses of the current  $I_h$  ( $\bar{g}_h = 1$  mS/cm $^2$ ) and of the activation variables  $F$  and  $S$  are displayed. The slow exponential time course of the variable  $S$  is followed by the current and the estimated time constant is of 3013.1 ms. (b) deactivation of  $I_h$ . Same protocol as in (a), except that the initial voltage is of  $-110$  mV. In this case, although the membrane is clamped to the same voltage as in (a), the current follows the faster time course of variable  $F$ , and a small time constant of 182.7 ms is measured. (c) time constants obtained for activation and deactivation of  $I_h$  as a function of the membrane potential. Circles indicate experimental data obtained by McCormick and Pape during activation (filled circles) and deactivation (open circles). Triangles represent time constants estimated from a single exponential fitting of currents illustrated in (a) and (b) (filled triangles = activation, open triangles = deactivation). Solid lines represent the functions used for modeling the time constants of  $I_h$  (cf Table 1).

perimental data points, the slow components of the time constant of activation are well represented in this model.

The time constant  $\tau_s(V)$  is chosen by an exponential fit of experimental data of activation, whereas  $\tau_f(V)$  is fitted as a bell-shaped function as close as possible to experimental data of deactivation process. These functions are listed in Table 1. We now investigate the oscillatory behavior seen in a single compartment model of the TC cell, including the model of  $I_h$  described above, as well as the leakage current, the low threshold current  $I_T$  and the slow potassium current  $I_{K2}$  (cf Materials and Methods).

*In vitro* experiments have shown that although some TC neurons are spontaneously oscillating, the presence and the pattern of oscillations strongly depends on  $I_h$ . Blocking  $I_h$  by application of caesium results in the abolition of slow oscillations and the membrane lies in a hyperpolarized resting potential.<sup>2,16</sup> On the other hand, enhancement of  $I_h$  by application of norepinephrine usually abolishes slow oscillations resulting in a depolarized resting potential, close to firing threshold.<sup>16,17</sup> Such a depolarized resting state is probably adequate for describing the relay mode of thalamic

cells. Moreover, for cat TC cells, spindle-like oscillations have also been found when enhancing  $I_h$ .<sup>16</sup> In this case, while increasing  $I_h$  strength, the following sequence of modes were observed: a hyperpolarized resting state when  $I_h$  is blocked, slow oscillations for weak values of  $I_h$ , spindle-like oscillations for higher values of  $I_h$  and finally, a depolarized resting state for a further increase in the value of  $I_h$ . This sequence was reversed by gradually decreasing the strength of  $I_h$ .

A similar sequence of oscillatory modes can be seen in the model as the maximal conductance of  $I_h$  is decreased. As shown in Figure 2, for the highest values of  $\bar{g}_h$ , the membrane lies in a depolarized resting state close to  $-60$  mV. Decreasing  $\bar{g}_h$  leads to spindle-like oscillations (intraspindle frequency of 10–14 Hz and a period of approximately 9 s). As  $\bar{g}_h$  is decreased further, one observes oscillations of a lower frequency around 1.1 Hz. Finally, for the weakest values of  $\bar{g}_h$ , the membrane switches to a hyperpolarized resting state, close to  $-80$  mV.

## Discussion

We have proposed a double activation model of the hyperpolarization-activated current  $I_h$ . This model accounts for voltage clamp data for this current while preserving the slow component of activation of the current, which would be lost in a single activation model. We believe that this slow component is important for the intrinsic properties of thalamocortical neurons. It must be pointed out that, in addition to thalamic cells,<sup>2,16</sup> such slow components have been observed during activation of a very similar current in crustacean motor neurons<sup>18</sup> and in sinoatrial node cells.<sup>19</sup>

The slow oscillations of TC cells are thought to depend on the interaction between  $I_T$  and  $I_h$ .<sup>2,16</sup> This hypothesis has been confirmed by modeling studies of these two currents.<sup>20–22</sup> The model proposed here for  $I_h$  also accounts for the production of such slow oscillations when combined with  $I_T$  (not shown). No spindle-like oscillations were reported in previous modeling studies, although some of them take into account a large variety of currents.<sup>20,22</sup> Oscillations endowed with some features of the spindle-like oscillations are observed when the double activation model of  $I_h$  is combined with  $I_T$  and the slow potassium current  $I_{K2}$ . In addition, it must be pointed out that when considering a single-activation model of  $I_h$  (cf reference 15), we were unable to find spindle-like oscillating behavior from the same combination of currents. One possible explanation is that for single activation models of  $I_h$ , the slow time constants of activation are not reproduced. It is likely that these components are essential for producing spindle-like behavior.

The main features of spindle-like oscillations are the presence of short bursts of calcium spikes lasting 2 to 5 s, long silent interbursts phases (5–25 s) during which

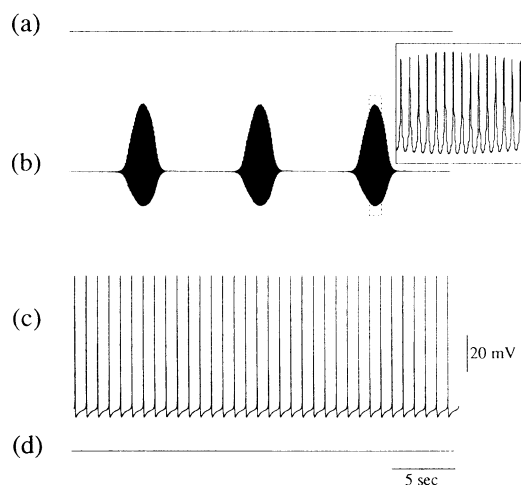


FIG. 2. Different types of oscillatory behavior obtained from the double activation model of  $I_b$ , combined with  $I_T$  and  $I_{K2}$ . The same values of the conductances of  $I_T$  and  $I_{K2}$  are used here ( $\bar{g}_T = 1.75$  mS/cm<sup>2</sup>,  $\bar{g}_{K2} = 3$  mS/cm<sup>2</sup>) and different modes can be seen for decreasing values of the maximal conductance of  $I_b$ . (a) depolarized resting state around  $-57$  mV for  $\bar{g}_b = 1$  mS/cm<sup>2</sup>, (b) spindle-like oscillations for  $\bar{g}_b = 0.4$  mS/cm<sup>2</sup>, (c) slow oscillations for  $\bar{g}_b = 0.002$  mS/cm<sup>2</sup>, (d) hyperpolarized resting state around  $-82$  mV for  $\bar{g}_b = 0$ . Inset in (b): oscillations delimited by the dashed line are shown at higher temporal resolution (magnification of 10).

the membrane slowly hyperpolarizes, and the transformation of spindle-like oscillations into slow oscillations following a depolarizing current step (not shown). However, the frequency of intraspindle oscillations is higher in the model than in experiments at the same temperature. Several modifications should improve this model. First, only three currents were included in our simulations. In the presence of other currents, such as the persistent sodium current<sup>6</sup> or other potassium currents,<sup>11</sup> spindle-like oscillations could occur at more hyperpolarized membrane potentials, where the kinetics of  $I_T$  are slower. Second, the effects of intracellular calcium have been neglected. Experiments on sino-atrial node cells<sup>23</sup> suggest that intracellular calcium shifts the voltage dependence of the activation function  $I_b$ . As this modulation occurs on relatively slow time scales, then if the same effect can be shown in TC cells, it could constitute an important element which might contribute to spindle-like oscillatory behavior.

Finally, TC cell simulations using the double activation model of  $I_b$  reproduce a similar sequence of

oscillating and resting states, as seen experimentally by the experiments of Soltesz *et al.*<sup>16</sup> The transition between these modes is achieved by increasing the maximal conductance of  $I_b$ . The model therefore produces several modes very similar to those seen in TC cells, and the transitions between them.

## Conclusions

The model of the hyperpolarization-activated inward current proposed here is based on the cooperation of two activation variables, and accounts for the unusual kinetic properties of this current. This model also preserves the slow components of activation of this current. Different types of oscillatory behavior are seen when combining this model of  $I_b$  with known models of two other currents of TC neurons, namely  $I_T$  and  $I_{K2}$ . Among these, are slow oscillations and spindle-like oscillations. The latter can be obtained only when considering the double activation model for  $I_b$ , which suggests that the slow components of the activation of  $I_b$  might be essential for reproducing spindle-like oscillatory behavior.

## References

1. Steriade M and Llinas RR. *Physiol Reviews* **68**, 649–742 (1988).
2. McCormick DA and Pape HC. *J Physiol* **431**, 291–318 (1990).
3. Leresche N, Lightowler S, Soltesz I *et al.* *J Physiol* **441**, 155–174 (1991).
4. Curro Dossi R, Nunez A and Steriade M. *J Physiol* **447**, 215–234 (1992).
5. Steriade M and Deschênes M. *Brain Res Reviews* **8**, 1–63 (1984).
6. Jahnsen H and Llinas RR. *J Physiol* **349**, 227–247 (1984).
7. Coulter DA, Huguenard JR and Prince DA. *J Physiol* **414**, 587–604 (1989).
8. Huguenard JR, Coulter DA and Prince DA. *J Neurophysiol* **66**, 1305–1315 (1991).
9. Huguenard JR and Prince DA. *J Neurophysiol* **66**, 1316–1328 (1991).
10. McCormick DA. *J Neurophysiol* **66**, 1176–1189 (1991).
11. Budde T, Mayer R and Pape HC. *Eur J Neurosci* **4**, 708–722 (1992).
12. Hodgkin AL and Huxley AF. *J Physiol* **117**, 500–544 (1952).
13. Jahnsen H and Llinas RR. *J Physiol* **349**, 205–226 (1984).
14. Wang XJ, Rinzel J and Rogawski MA. *J Neurophysiol* **66**, 839–850 (1991).
15. Huguenard JR and McCormick DA. *J Neurophysiol* **68**, 1373–1383 (1992).
16. Soltesz I, Lightowler S, Leresche N *et al.* *J Physiol* **441**, 175–197 (1991).
17. McCormick DA and Pape HC. *J Physiol* **431**, 319–342 (1990).
18. Kiehn O and Harris-Warrick RM. *J Neurophysiol* **68**, 496–508 (1992).
19. van Ginneken ACG and Giles W. *J Physiol* **434**, 57–83 (1991).
20. Lytton W and Sejnowski T.J. *J Neurophysiol* **66**, 1059–1079 (1991).
21. Toth T and Crunelli V. *NeuroReport* **3**, 65–68 (1992).
22. McCormick DA and Huguenard JR. *J Neurophysiol* **68**, 1384–1400 (1992).
23. Hagiwara N and Irishawa H. *J Physiol* **409**, 121–141 (1989).

ACKNOWLEDGEMENTS: This research was partly supported by the Belgian Government (ARC and IM-PULS, project RFO AI 10), and by the E.E.C. (ESPRIT, Basic Research, project 3234). We acknowledge Drs Diego Contreras, David McCormick, Terrence Sejnowski and Mircea Steriade for stimulating discussions.

Received 26 November 1992;  
accepted 2 December 1992